Tracking a Ballistic Target: Comparison of Several Nonlinear Filters

A. FARINA, Fellow, IEEE
Alenia Marconi Systems
Italy

B. RISTIC
Defence Science and Technology Organisation
Australia

D. BENVENUTI
Alenia Marconi Systems
Italy

This paper studies the problem of tracking a ballistic object in the reentry phase by processing radar measurements. A suitable (highly nonlinear) model of target motion is developed and the theoretical Cramer–Rao lower bounds (CRLB) of estimation error are derived. The estimation performance (error mean and standard deviation; consistency test) of the following nonlinear filters is compared: the extended Kalman filter (EKF), the statistical linearization, the particle filtering, and the unscented Kalman filter (UKF). The simulation results favor the EKF; it combines the statistical efficiency with a modest computational load. This conclusion is valid when the target ballistic coefficient is a priori known.

Manuscript received April 20, 2001; revised January 24, 2002;. released for publication April 8, 2002.

IEEE Log No. T-AES/38/3/06432.

Refereeing of this contribution was handled by P. Willett.

Authors' addresses: A. Farina and D. Benvenuti, Alenia Marconi Systems, Radar & Technology Division, Via Tiburtina Km. 12.400, 00131 Rome, Italy, E-mail: (afarina(dbenvenuti)@amsjv.it); B. Ristic, Surveillance Systems Division, Defence Science and Technology Organisation, PO Box 1500, Salisbury, SA 5108, Australia.

0018-9251/02/$17.00 © 2002 IEEE

I. NOMENCLATURE

$\bar{\varepsilon}_k$	Average NEES at time instant k
$\mathbf{e}_k$	State estimation error at time instant k, dim(4,1)
$\mathbf{f(s)}$	Nonlinearity function in the dynamic state equation, dim(2,1),
g	9.81 m/s^2 gravity acceleration
$\mathbf{H}$	Matrix in radar measurement equation, dim(2,4)
$\mathbf{K}_k$	Kalman gain matrix, dim(4,2)
n	Number of particles in PF
$\mathbf{N}_{\mathbf{f},k}$	Matrix needed to approximate (in the linear statistic fashion) the nonlinearity $\mathbf{f(s)}$, dim(2,4)
$p(\mathbf{s}_k \mid \mathbf{z}_1,\ldots,\mathbf{z}_k)$	Posterior pdf of state vector
$p_N(\mathbf{s};\hat{\mathbf{s}},\mathbf{P})$	Multidimensional Gaussian pdf with mean $\hat{\mathbf{s}}$ and covariance matrix $\mathbf{P}$ calculated at $\mathbf{s}$
$q_{k+1}(i)$	Normalized weights for PF
q	Intensity of process noise in target model
$\mathbf{Q}$	Covariance matrix of process noise in target model, dim(4,4)
$\mathbf{R}_k$	Covariance matrix of measurement error, dim(2,2)
$\mathbf{s}_k$	Target state at time instant k, dim(4,1)
$\hat{\mathbf{s}}_{k+1\|k},\mathbf{P}_{k+1\|k}$	One-step ahead predicted state and corresponding covariance matrix, dim(4,1) and dim(4,4) respectively
$\hat{\mathbf{s}}_{k\|k},\mathbf{P}_{k\|k}$	Filtered state and corresponding covariance matrix
T	Time interval between radar measurements
v	Module of target velocity
$\mathbf{v}_k$	Measurement error on the Cartesian coordinates, dim(2,1)
x	Target abscissa
y	Target ordinate
x_0,y_0	Target coordinates at time t_0
x_R,y_R	Radar coordinates
$\mathbf{z}_k$	Radar measurement vector, dim(2,1)
$\mathbf{Z}_k = \{\mathbf{z}_1,\ldots,\mathbf{z}_k\}$	Collection of all radar measurements up to time k
β	Ballistic coefficient of target
$\mathbf{\Phi}$	Transition matrix of target state equation, dim(4,4)
γ	Angle between horizontal axis and direction of target motion
κ	Scaling parameter of UKF
ρ	Air density
σ_r, σ_ε	Error standard deviations of radar measurements for range and elevation angle, respectively

$\sigma_d^2, \sigma_h^2, \sigma_{dh}$	Variance of measurement errors in Cartesian coordinates (abscissa, ordinate) and their cross-covariance, respectively
$\Sigma_k = \{\mathbf{s}_k(i) : i = 1,\ldots n\}$	Set of random samples (particles)
$\mathbf{J}_{k+1}$	Information matrix, dim(4,4)
$\mathbf{\Psi}_k$, $\mathbf{F}_k$	Jacobians, dim(4,4) and dim(2,4), respectively
$\xi_{k\|k}(i)$, $\zeta_{k\|k}(i)$, W_i	Sigma points and weights for UKF.

II. INTRODUCTION

The problem of tracking ballistic objects in the reentry phase has attracted much attention of the researchers for both theoretical and practical reasons. Technically speaking we need to set up a stochastic nonlinear filter due to the nonlinearity of the dynamic state equation of the target; tracking filters have been conceived for this purpose since the early days of the invention of the Kalman filter [12]: see for instance [13, 18, 3]. More recently, the following papers have been published on this subject: [4, 11, 15]. Practical applications are in the fields of surveillance for defense and for safety against the reentry of old satellites. In relation to the second application, it is known that the number of objects orbiting the Earth has been continuously increasing since the launch of the first satellite in 1957. They are old satellites, pieces of satellites due to explosion and erosion, upper stages of missiles, etc. It is relevant to have means to detect, classify, and track these pieces of debris [2]; big objects that reenter the atmosphere should be accurately tracked to anticipate their landing points on Earth. The aim of our study is to formulate the nonlinear tracking filtering problem and to discuss the application of several approximate filters.

Section III provides the models of kinematics of the target and of the radar measurements. The Cramer–Rao lower bound (CRLB) for nonlinear discrete-time filtering problems is discussed in Section IV. The four tracking filters to compare are as follows.

1) the extended Kalman filter (EKF),
2) the statistical linearization also referred to as CADET (Covariance Analysis DEscribing function Technique) developed in the past by The Analytic Sciences Corporation (TASC) [9],
3) the recently conceived unscented Kalman filter (UKF) [15],
4) the particle filter (PF) [10].

These approximate techniques are discussed in Section V. Every filter needs to be compared with the CRLB. Results concerning the simulation of the tracking filters, error analysis, comparison with the CRLB and consistency tests are presented in Section VI. Our conclusions are collected in Section VII. The contribution of this work to the state of the art is to have compared the performance of two popular (the EKF and the CADET) and two modern (the PF and the UKF) trackers to the CRLB. Recommendations to select the best filter in terms of performance and computational cost are also given. A note on the mathematical symbols; bold capitol letters represent matrices, bold lower case letters denote vectors; the apex T in $[\bullet]^T$ stands for transposition of either a matrix or a vector; $E\{\bullet\}$, $\overline{(\bullet)}$ denote the expectation operator; $\mathbf{x}[i]$ and $\mathbf{A}[i,j]$ are, respectively, the ith entry of vector $\mathbf{x}$ and the ijth entry of matrix $\mathbf{A}$.

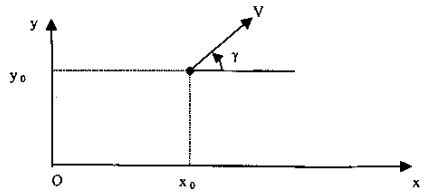

Fig. 1. Coordinate reference system.

III. MODELS OF TARGET MOTION AND OF RADAR MEASUREMENTS

Consider an object which is launched from one point on Earth to another point along a ballistic flight. The kinematics of the ballistic object in the reentry phase is derived under the following hypotheses. The forces acting on the target are gravity, and drag. The effects of centrifugal acceleration, Coriolis acceleration, wind, lift force, and spinning motion are ignored, due to their small effect on the trajectory. Another simplifying assumption is related to flat Earth approximation.

Having assumed a flat Earth, an orthogonal coordinate reference system can be used with the following variables (Fig. 1):

x is the abscissa,
y is the ordinate,
x_0 and y_0 are the target coordinates at time t_0,
v is the velocity module,
γ is the angle between the horizontal axis and the direction of motion.

The target motion is described by the following discrete-time nonlinear dynamic state equation

$$\mathbf{s}_{k+1} = \psi_k(\mathbf{s}_k) + \mathbf{G}\begin{bmatrix} 0 \\ -g \end{bmatrix} + \mathbf{w}_k \tag{1}$$

where the state vector is

$$\mathbf{s}_k \triangleq [x_k \quad \dot{x}_k \quad y_k \quad \dot{y}_k]^T \tag{2}$$

and

$$\psi_k(\mathbf{s}_k) = \mathbf{\Phi}\mathbf{s}_k + \mathbf{G}\mathbf{f}_k(\mathbf{s}_k) \tag{3}$$

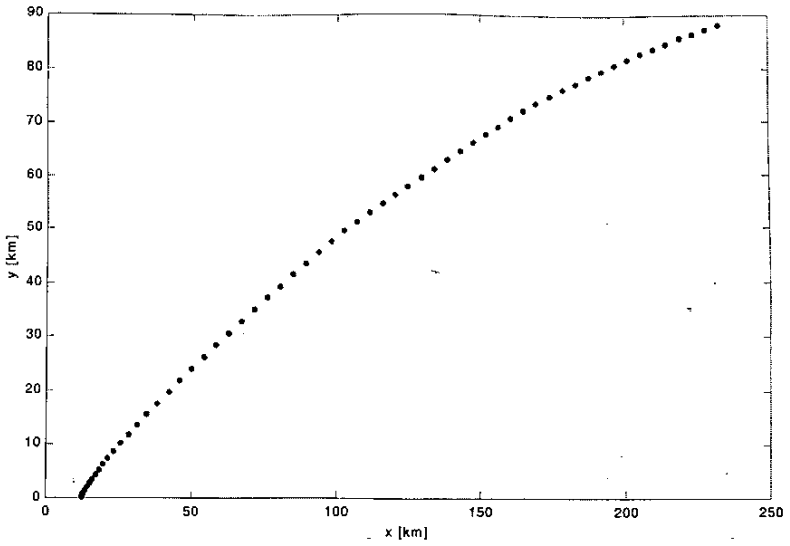

Fig. 2(a). Example of target trajectory.

$$\mathbf{\Phi} \triangleq \begin{bmatrix} 1 & T & 0 & 0 \\ 0 & 1 & 0 & 0 \\ 0 & 0 & 1 & T \\ 0 & 0 & 0 & 1 \end{bmatrix} \tag{4}$$

$$\mathbf{G} \triangleq \begin{bmatrix} \frac{T^2}{2} & 0 \\ T & 0 \\ 0 & \frac{T^2}{2} \\ 0 & T \end{bmatrix} \tag{5}$$

where T is the time interval between the radar measurements. The drag is a force directed in opposition to the target speed and with an intensity equal to $\frac{1}{2}(g/\beta)\rho v^2$ [25]; being: g the gravity acceleration, β[1] the ballistic coefficient, ρ the air density (typically it is an exponentially decaying function of height, $\rho = c_1 e^{-c_2 y}$ where $c_1 = 1.227$, $c_2 = 1.09310^{-4}$ for $y < 9144$ m, and $c_1 = 1.754$, $c_2 = 1.4910^{-4}$ for $y \geq 9144$ m) and v the module of target velocity. In terms of state vector components, the drag is

$$\mathbf{f}_k(\mathbf{s}_k) = -0.5\frac{g}{\beta}\rho(\mathbf{s}_k[3])(\mathbf{s}_k^2[2] + \mathbf{s}_k^2[4]) \times \begin{bmatrix} \cos\left(\text{arctg}\left(\frac{\mathbf{s}_k[4]}{\mathbf{s}_k[2]}\right)\right) \\ \sin\left(\text{arctg}\left(\frac{\mathbf{s}_k[4]}{\mathbf{s}_k[2]}\right)\right) \end{bmatrix}. \tag{6}$$

[1]It depends on the target mass, the body shape, and the cross-sectional area of the target perpendicular to the direction of motion. It is constant for high super-sonic speed, while due to the formation of shock waves, it diminishes when target velocity approaches Mach 1. In our study case (see Fig. 2(a)) the speed tends to Mach 1 just at the end of the trajectory, so the approximation done (i.e.: β = constant) is quite good.

By exploiting the following identities

$$\cos\left(\text{arctg}\left(\frac{y}{x}\right)\right) = \frac{x}{\sqrt{x^2+y^2}} \qquad \sin\left(\text{arctg}\left(\frac{y}{x}\right)\right) = \frac{y}{\sqrt{x^2+y^2}} \tag{7}$$

(6) can be rewritten as follows

$$\mathbf{f}_k(\mathbf{s}_k) = -0.5\frac{g}{\beta}\rho(\mathbf{s}_k[3])\sqrt{\mathbf{s}_k^2[2] + \mathbf{s}_k^2[4]}\begin{bmatrix} \mathbf{s}_k[2] \\ \mathbf{s}_k[4] \end{bmatrix}. \tag{8}$$

Process noise $\mathbf{w}_k$ in (1) is modeled as a zero-mean white Gaussian process with nonsingular covariance matrix

$$\mathbf{Q} = q\begin{bmatrix} \theta & \underline{0} \\ \underline{0} & \theta \end{bmatrix}, \qquad \text{with} \quad \theta = \begin{bmatrix} \frac{T^3}{3} & \frac{T^2}{2} \\ \frac{T^2}{2} & T \end{bmatrix} \tag{9}$$

where q is a parameter related to process noise intensity [1, p. 262]. The process noise accounts for all forces that have not been considered in the model and possible deviations of the model from the reality.

An example of a target trajectory is shown in the following figure; the relevant parameters are: $\beta = 40000$ Kg $\cdot$ m^{-1} $\cdot$ s^{-2}, $q = 1$ m^2 $\cdot$ s^{-3}, $T = 2$ s, $y_0 = 88$ km, $x_0 = 232$ km, $\gamma_0 = 190°$, $v_0 = 2290$ m/s, number of path samples $N = 60$. Fig. 2(a) shows the trajectory in the x-y plane, while Fig. 2(b) depicts the speed and acceleration of target versus time; the strong target deceleration due to drag is apparent.

The measurements, collected by the radar for target tracking, are the range r and elevation ε; the radar is located at $x_R = 0$, $y_R = 0$ in all the numerical evaluations here. The error standard deviations of these measurements are denoted as σ_r (for range)

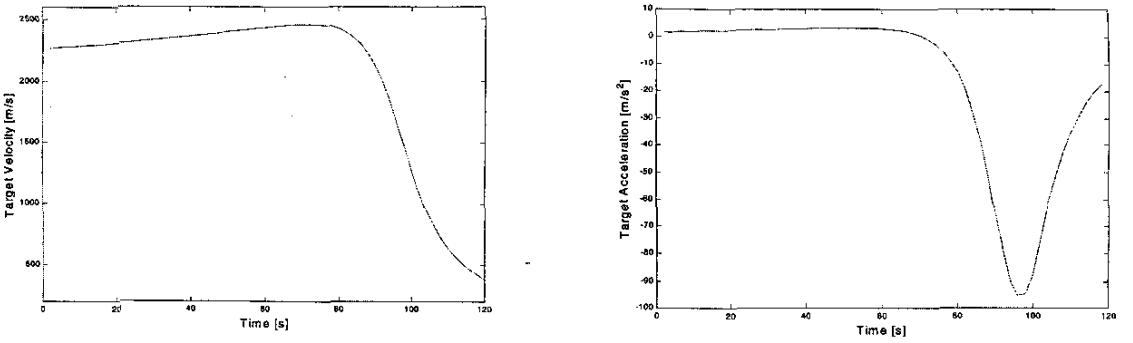

Fig. 2(b). Speed and acceleration of target versus time for trajectory of Fig. 2(a).

and σ_ε (for elevation). Radar measurements are transformed to the Cartesian coordinates $d = r\cos\varepsilon$ and $h = r\sin\varepsilon$ (for measured target abscissa and ordinate) so that the measurement equation is linear

$$\mathbf{z}_k = \mathbf{H}\mathbf{s}_k + \mathbf{v}_k \tag{10}$$

where

$$\mathbf{z}_k = [d_k \;\; h_k]^{\mathrm{T}}, \qquad \mathbf{H} = \begin{pmatrix} 1 & 0 & 0 & 0 \\ 0 & 0 & 1 & 0 \end{pmatrix}.$$

$\mathbf{v}_k$ is the noise on the measured Cartesian coordinates; it is independent of the process noise $\mathbf{w}_k$; it is zero-mean white Gaussian with covariance matrix $\mathbf{R}_k$ [8, p. 155] with elements:

$$\begin{aligned} \sigma_d^2 &= \sigma_r^2\cos^2(\varepsilon) + r^2\sigma_\varepsilon^2\sin^2(\varepsilon) \\ \sigma_h^2 &= \sigma_r^2\sin^2(\varepsilon) + r^2\sigma_\varepsilon^2\cos^2(\varepsilon) \\ \sigma_{dh} &= (\sigma_r^2 - r^2\sigma_\varepsilon^2)\sin(\varepsilon)\cos(\varepsilon). \end{aligned} \tag{11}$$

For all practical purposes this is a good approximation[2] which greatly simplifies the tracking algorithm; otherwise one would also have to take into consideration the nonlinearity of the measurement equation.

IV. CRAMER–RAO LOWER BOUND FOR BALLISTIC TARGET TRACKING

The objective of this section is to derive the theoretical CRLB of the variance of estimation error for the nonlinear dynamic system described by (1) to (11). The optimal estimator for this problem cannot be built and hence we resort to approximate filters described in Section V. The theoretical lower bound, which defines the best achievable performance, plays an important role in algorithm evaluation and assessment of the level of approximation introduced in the filtering algorithms.

[2]The unbiased and consistent conversion of measurements is described in [16]. According to [16], the measurement conversion given by (10) and (11) is unbiased if $r\sigma_\varepsilon^2/\sigma_r < 0.4$ and if $\sigma_\varepsilon < 23°$. Both of these conditions are satisfied in the present study (see Section VI) and therefore the conclusions achieved are valid.

A. General Framework for CRLB Derivation

The general framework for derivation of CRLB of an unbiased estimator for non linear discrete-time system is described in [23]. The sequence of information matrices obeys the following recursion

$$\mathbf{J}_{k+1} = \mathbf{D}_k^{22} - \mathbf{D}_k^{21}(\mathbf{J}_k + \mathbf{D}_k^{11})^{-1}\mathbf{D}_k^{12} \tag{12}$$

where for the case of additive Gaussian noise, as in (1), and for the linear measurement equation as in (10), we have that

$$\mathbf{D}_k^{11} = E\{\Psi_k^T\mathbf{Q}^{-1}\Psi_k\} \tag{13}$$

$$\mathbf{D}_k^{12} = -E\{\Psi_k^T\}\mathbf{Q}^{-1} = [\mathbf{D}_k^{21}]^{\mathrm{T}} \tag{14}$$

$$\mathbf{D}_k^{22} = \mathbf{Q}^{-1} + E\{\mathbf{H}^T\mathbf{R}_{k+1}^{-1}\mathbf{H}\} \tag{15}$$

with Jacobian Ψ_k defined as

$$\Psi_k = [\nabla_{\mathbf{s}_k}\psi_k^T(\mathbf{s}_k)]^{\mathrm{T}} \tag{16}$$

where $[\nabla_{\mathbf{s}_k}\psi_k^T(\mathbf{s}_k)]$ indicates the matrix of the first partial derivatives of the vector ψ_k^T (see (3)) with respect to the state vector $\mathbf{s}_k$. Note that Jacobian Ψ_k is evaluated at the true target state. Substitution of (13)–(15) into (12) yields the following recursion

$$\begin{aligned} \mathbf{J}_{k+1} = \mathbf{Q}^{-1} + E\{\mathbf{H}^T\mathbf{R}_{k+1}^{-1}\mathbf{H}\} - \mathbf{Q}^{-1}E\{\Psi_k\} \\ \cdot[\mathbf{J}_k + E\{\Psi_k^T\mathbf{Q}^{-1}\Psi_k\}]^{-1}\cdot E\{\Psi_k^T\}\mathbf{Q}^{-1}. \end{aligned} \tag{17}$$

The CRLB of an unbiased estimate of the state vector at time index k is then [24]

$$\mathrm{CRLB}\{\mathbf{s}_k[j]\} = \mathbf{J}_k^{-1}[j,j], \qquad \text{for} \quad j = 1,2,3,4. \tag{18}$$

In the absence of process noise, the recursive equation for computation of information matrix $\mathbf{J}_k$ follows from [22]

$$\mathbf{J}_{k+1} = (\Psi_k^{-1})^T\mathbf{J}_k\Psi_k^{-1} + \mathbf{H}^T\mathbf{R}_{k+1}^{-1}\mathbf{H}. \tag{19}$$

Note that (19) is identical in form to the EKF inverse covariance matrix propagation in absence of process noise. The difference is that Jacobian Ψ_k in the calculation of information matrix is evaluated at

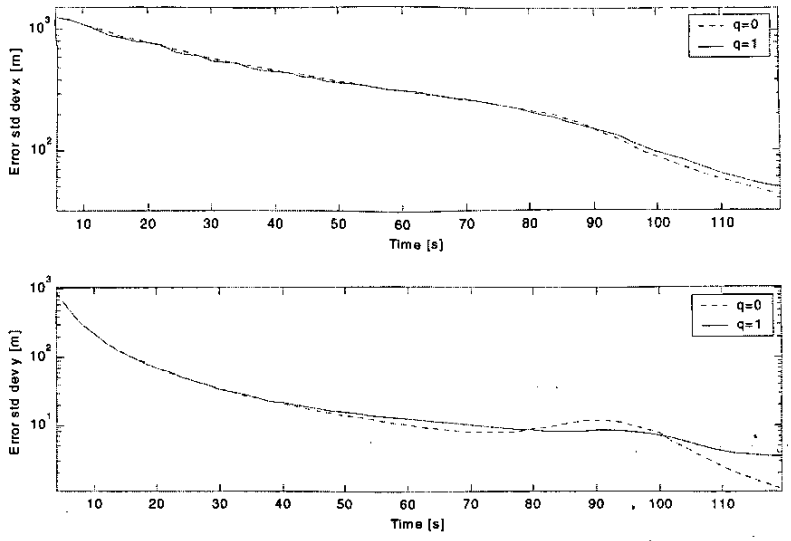

Fig. 3. Influence of process noise intensity q on CRLB for target position $\mathbf{s}_k[1] = x_k$ and $\mathbf{s}_k[3] = y_k$.

the *true* target state, while in the covariance matrix propagation of the EKF it is evaluated at the *estimated* target state.

The initial information matrix $\mathbf{J}_0$ is calculated as the inverse of initial covariance matrix

$$\mathbf{J}_0 = \mathbf{P}_{0|0}^{-1} \tag{20}$$

where the initial covariance matrix corresponds to the two-point differencing method of filter initialization [8, p. 228], [1, p. 253]. A suitable expression for $\mathbf{P}_{0|0}$ is as follows

$$\mathbf{P}_{0|0} = \begin{bmatrix} \sigma_d^2 & -\frac{\sigma_d^2}{T} & \sigma_{dh} & -\frac{\sigma_{dh}}{T} \\ -\frac{\sigma_d^2}{T} & 2\frac{\sigma_d^2}{T^2} & -\frac{\sigma_{dh}}{T} & 2\frac{\sigma_{dh}}{T^2} \\ \sigma_{dh} & -\frac{\sigma_{dh}}{T} & \sigma_h^2 & -\frac{\sigma_h^2}{T} \\ -\frac{\sigma_{dh}}{T} & 2\frac{\sigma_{dh}}{T^2} & -\frac{\sigma_h^2}{T} & 2\frac{\sigma_h^2}{T^2} \end{bmatrix} \tag{21}$$

which derives from the expression of $\mathbf{s}_{0|0}$

$$\mathbf{s}_{0|0}^T = \begin{bmatrix} x_2 & \frac{x_2 - x_1}{T} & y_2 & \frac{y_2 - y_1}{T} \end{bmatrix}. \tag{22}$$

B. Derivation of Jacobian and an Example

From (16) and (3) it follows that Jacobian $\mathbf{\Psi}_k$ can be written as

$$\mathbf{\Psi}_k = \mathbf{\Phi} + \mathbf{G}\mathbf{F}_k \tag{23}$$

where the elements of

$$\mathbf{F}_k = [\nabla_{\mathbf{s}_k} \mathbf{f}_k^T(\mathbf{s}_k)]^T \tag{24}$$

are as follows

$$\begin{aligned}
\mathbf{F}_k[1,1] &= 0 \\
\mathbf{F}_k[2,1] &= 0 \\
\mathbf{F}_k[1,2] &= -\frac{1}{2}\cdot\frac{g}{\beta}\cdot\rho_k\cdot\frac{2(\mathbf{s}_k[2])^2 + (\mathbf{s}_k[4])^2}{\sqrt{(\mathbf{s}_k[2])^2 + (\mathbf{s}_k[4])^2}} \\
\mathbf{F}_k[2,2] &= \mathbf{F}_k[1,4] \\
\mathbf{F}_k[1,3] &= \frac{1}{2}\cdot\frac{g}{\beta}\cdot c_2\rho_k\cdot\mathbf{s}_k[2]\sqrt{(\mathbf{s}_k[2])^2 + (\mathbf{s}_k[4])^2} \\
\mathbf{F}_k[1,4] &= -\frac{1}{2}\cdot\frac{g}{\beta}\cdot\rho_k\cdot\frac{\mathbf{s}_k[2]\cdot\mathbf{s}_k[4]}{\sqrt{(\mathbf{s}_k[2])^2 + (\mathbf{s}_k[4])^2}} \\
\mathbf{F}_k[2,3] &= \frac{1}{2}\cdot\frac{g}{\beta}\cdot c_2\rho_k\cdot\mathbf{s}_k[4]\sqrt{(\mathbf{s}_k[2])^2 + (\mathbf{s}_k[4])^2} \\
\mathbf{F}_k[2,4] &= -\frac{1}{2}\cdot\frac{g}{\beta}\cdot\rho_k\cdot\frac{2(\mathbf{s}_k[4])^2 + (\mathbf{s}_k[2])^2}{\sqrt{(\mathbf{s}_k[2])^2 + (\mathbf{s}_k[4])^2}}.
\end{aligned} \tag{25}$$

The estimate of the air density in (25) is given by

$$\rho_k = c_1 e^{-c_2 \mathbf{s}_k[3]}. \tag{26}$$

Jacobian $\mathbf{\Psi}_k$ depends on the target state vector, hence the expectations in (17) are taken over ensemble of $\mathbf{s}_k$ (which is random due to process noise). The implementation of recursion (17) is based on Monte Carlo averaging over multiple realizations of the target trajectory. Fig. 3 displays in the log-scale the square root of the CRLB for the target position $\mathbf{s}_k[1] = x_k$, $\mathbf{s}_k[3] = y_k$, i.e., $\sqrt{\text{CRLB}\{\mathbf{s}_k[1]\}}$, $\sqrt{\text{CRLB}\{\mathbf{s}_k[3]\}}$ in absence and in presence of process noise $\mathbf{w}_k$ in the

state equation (1). The parameters are as for Fig. 2, and in addition $\sigma_r = 100$ m and $\sigma_\epsilon = 0.017$ rad. The CRLB in the presence of process noise ($q = 1$ case) was obtained by averaging over 100 Monte Carlo runs. In absence of process noise the CRLB was calculated using recursion of (19), where no averaging is required. Observe from Fig. 3 that the CRLB on the target position coordinates x and y, in the presence of a modest amount of process noise, is practically equal to the CRLB in absence of noise; only at the end of the observation period the two curves differ a little bit.

V. TRACKING FILTERS

In this section we describe four recursive estimators (filters) to be used for tracking a ballistic object. These filters determine in approximate way the mean and covariance matrix of the probability of target state conditioned to the measured radar data: $p(\mathbf{s}_k \mid \mathbf{Z}_k)$ which is the probability density function (pdf) of the vector $\mathbf{s}_k$ given the set $\mathbf{Z}_k \triangleq \{\mathbf{z}_1, \mathbf{z}_2, \ldots, \mathbf{z}_k\}$ of all measurements up to kth time instant. These filters are the EKF, the CADET, the KF, and the PF. All of them are based on approximations and our goal is to assess the influence of a particular approximation on the tracking accuracy. The filters are initialized using the same two-point differencing method [8, p. 228], [1, p. 253], to match the computation of the CRLB.

A. Application of EKF

See, for instance, [8, pp. 113–116] for details. The prediction at time instant $k+1$ given all the measurements up to time instant k is carried out as follows

$$\begin{aligned} \hat{\mathbf{s}}_{k+1|k} &= \psi_k(\hat{\mathbf{s}}_{k|k}) + \mathbf{G}\begin{pmatrix} 0 \\ -g \end{pmatrix} \\ \mathbf{P}_{k+1|k} &= (\Phi + \mathbf{G}\cdot\mathbf{F}_k)\mathbf{P}_{k|k}(\Phi + \mathbf{G}\cdot\mathbf{F}_k)^T + \mathbf{Q} \end{aligned} \tag{27}$$

where Φ and $\mathbf{G}$ are given by (4) and (5), while $\mathbf{F}_k$ is the Jacobian (see equations (25)) calculated at the estimated state $\hat{\mathbf{s}}_{k|k}$. The estimation at time instant $k+1$ given all the measurements up to time instant $k+1$ can be done after calculating the Kalman gain

$$\mathbf{K}_{k+1} = \mathbf{P}_{k+1|k}\mathbf{H}^T(\mathbf{H}\mathbf{P}_{k+1|k}\mathbf{H}^T + \mathbf{R}_k)^{-1} \tag{28}$$

by the equations

$$\begin{aligned} \hat{\mathbf{s}}_{k+1|k+1} &= \hat{\mathbf{s}}_{k+1|k} + \mathbf{K}_{k+1}(\mathbf{z}_{k+1} - \mathbf{H}\hat{\mathbf{s}}_{k+1|k}) \\ \mathbf{P}_{k+1|k+1} &= (\mathbf{I} - \mathbf{K}_{k+1}\mathbf{H})\mathbf{P}_{k+1|k}. \end{aligned} \tag{29}$$

The EKF only uses the first order terms in the Taylor series expansion of the nonlinear state equation. In general, when the filtering problem is highly nonlinear and the local linearity assumption breaks down, the EKF may introduce large estimation errors due to filter divergence.

B. Application of CADET

With this approach, instead of calculating the derivative (24) once (as in the EKF), the coefficients of the linear expression

$$\mathbf{f}(\mathbf{s}) \cong \mathbf{N}_\mathbf{f}\mathbf{s} + \mathbf{f}_0 \tag{30}$$

are found by minimizing the mean of the squared error [9], [8, pp. 117–121]

$$e = [\mathbf{f}(\mathbf{s}) - \mathbf{f}_0 - \mathbf{N}_\mathbf{f}\mathbf{s}]^T[\mathbf{f}(\mathbf{s}) - \mathbf{f}_0 - \mathbf{N}_\mathbf{f}\mathbf{s}] \tag{31}$$

at each iteration of the filter. CADET tries to approximate the nonlinearity $\mathbf{f}_k(\mathbf{s}_k)$ of (3) with a linearity whose slope depends upon the variance of input stochastic process $\mathbf{s}_k$. By doing the calculations the following expressions are found

$$\begin{aligned} \mathbf{f}_k(\mathbf{s}_k) &= E\{\mathbf{f}_k(\mathbf{s}_k)\} + \mathbf{N}_{\mathbf{f},k}(\mathbf{s}_k - E\{\mathbf{s}_k\}) \\ &= \overline{\mathbf{f}_k(\mathbf{s}_k)} + \mathbf{N}_{\mathbf{f},k}(\mathbf{s}_k - \overline{\mathbf{s}_k}) \end{aligned} \tag{32}$$

with

$$\begin{aligned} \mathbf{N}_{\mathbf{f},k} &= [E\{\mathbf{f}_k(\mathbf{s}_k)\mathbf{s}_k^T\} - E\{\mathbf{f}_k(\mathbf{s}_k)\}E\{\mathbf{s}_k\}]\mathrm{cov}^{-1}(\mathbf{s}_k) \\ &= [\overline{\mathbf{f}_k(\mathbf{s}_k)\mathbf{s}_k^T} - \overline{\mathbf{f}_k(\mathbf{s}_k)}\,\overline{\mathbf{s}_k}]\mathrm{cov}^{-1}(\mathbf{s}_k) \end{aligned} \tag{33}$$

being $\mathrm{cov}^{-1}(\mathbf{s})$ the inverse of the covariance matrix of the vector $\mathbf{s}$. To design a suboptimal filter, it is necessary to specify how the following quantities: $E\{\mathbf{f}_k(\mathbf{s}_k)\mathbf{s}_k^T\}$, $E\{\mathbf{f}_k(\mathbf{s}_k)\}$ and $E\{\mathbf{s}_k\}$ are computed. In principle, they could be obtained by the knowledge of posterior density $p(\mathbf{s}_k \mid \mathbf{Z}_k)$ which is not known. The approximation made is to assume that this pdf is Gaussian so that only the mean and covariance matrix are needed; these, in turn, are substituted by $\hat{\mathbf{s}}_{k|k}$ and $\mathbf{P}_{k|k}$ provided by the filter. Thus, the CADET approach is similar in some aspect to the EKF, but more accurate and complex. In fact, it requires the calculation of the four-fold integrals

$$\begin{aligned} \overline{\mathbf{f}_k}(\hat{\mathbf{s}}_{k|k}) &\equiv \int \mathbf{f}(\mathbf{s}) p_N(\mathbf{s}; \hat{\mathbf{s}}_{k|k}, \mathbf{P}_{k|k}) d\mathbf{s}\Big|_{\hat{\mathbf{s}}_{k|k}} \quad \text{and} \\ \overline{\mathbf{f}_k(\hat{\mathbf{s}}_{k|k})\hat{\mathbf{s}}_{k|k}^T} &\equiv \int \mathbf{f}(\mathbf{s})\mathbf{s}^T p_N(\mathbf{s}; \hat{\mathbf{s}}_{k|k}, \mathbf{P}_{k|k}) d\mathbf{s}\Big|_{\hat{\mathbf{s}}_{k|k}} \end{aligned} \tag{34}$$

where $p_N(\mathbf{s}; \hat{\mathbf{s}}_{k|k}, \mathbf{P}_{k|k})$ is the multidimensional Gaussian pdf with mean $\hat{\mathbf{s}}_{k|k}$ and covariance matrix $\mathbf{P}_{k|k}$ calculated in the value $\mathbf{s}$.

The prediction equations of the filter take the form

$$\begin{aligned} \hat{\mathbf{s}}_{k+1|k} &= \psi_k(\hat{\mathbf{s}}_{k|k}) + \mathbf{G}\begin{bmatrix} 0 \\ -g \end{bmatrix} \\ \mathbf{P}_{k+1|k} &= (\Phi + \mathbf{G}\cdot\mathbf{N}_{\mathbf{f},k})\mathbf{P}_{k|k}(\Phi + \mathbf{G}\cdot\mathbf{N}_{\mathbf{f},k})^{\mathrm{T}} + \mathbf{Q} \end{aligned} \tag{35}$$

with

$$\mathbf{N}_{f,k} = [\overline{\mathbf{f}_k(\hat{\mathbf{s}}_{k|k})\hat{\mathbf{s}}_{k|k}^T} - \overline{\mathbf{f}_k(\hat{\mathbf{s}}_{k|k})}\,\overline{\hat{\mathbf{s}}_{k|k}}]\mathbf{P}_{k|k}^{-1}.$$

$\hat{\mathbf{s}}_{k|k}$ and $\mathbf{P}_{k|k}$ are given by the equations (29); the equation (28) provides the Kalman gain $\mathbf{K}_k$.

The four-fold integrals in (34) have been calculated as four-fold summations over a four-fold interval $\left[-5\sqrt{\mathbf{P}_{k/k}[i,i]}, 5\sqrt{\mathbf{P}_{k/k}[i,i]}\right]$ for $i = 1,2,3,4$ with step of $0.5\sqrt{\mathbf{P}_{k/k}[i,i]}$. This means that we need to calculate 21 points for each variable of the integral; overall for the four variables the number of summations to calculate is $21^4 = 195000$.

C. Application of Unscented KF (UKF)

Same as the EKF, the UKF is a recursive MMSE (minimum mean square error) estimator. But unlike the EKF, the UKF [14] does not approximate the nonlinear state and measurement equations. It uses the true nonlinear model of state and/or measurement equation but approximates the pdf of the state vector. This density is still Gaussian, but is specified by a set of deterministically chosen sample (or *sigma*) points. The sigma points completely capture the true mean and covariance of the Gaussian density and when propagated through the nonlinear system, capture the posterior mean and covariance accurately to the second order for any nonlinearity [15].

The unscented transform (UT) is a method for calculating the statistics of a random vector that undergoes a nonlinear transformation. Let $\mathbf{x}$ be the n_x dimensional random vector, $\mathbf{g}: R^{n_x} \mapsto R^{n_y}$ a nonlinear function and $\mathbf{y} = \mathbf{g}(\mathbf{x})$. Assume the mean and the covariance of $\mathbf{x}$ are $\overline{\mathbf{x}}$ and $\mathbf{P}_x$, respectively. The simple procedure for the calculation of the first two moments of $\mathbf{y}$ using the UT is as follows.

1) Compute $(2n_x + 1)$ sigma points[3] χ_i and their weights W_i

$$\begin{aligned}
&\chi_0 = \overline{\mathbf{x}} \quad W_0 = \kappa/(n_x + \kappa) \qquad i = 0\\
&\chi_i = \overline{\mathbf{x}} + \left(\sqrt{(n_x + \kappa)\mathbf{P}_x}\right)_i \qquad W_i = 1/[2(n_x + 1)] \qquad i = 1,\ldots,n_x\\
&\chi_i = \overline{\mathbf{x}} - \left(\sqrt{(n_x + \kappa)\mathbf{P}_x}\right)_i \qquad W_i = 1/[2(n_x + 1)] \qquad i = n_x + 1,\ldots,2n_x
\end{aligned} \tag{36}$$

where κ is a scaling parameter and $\left(\sqrt{(n_x + \kappa)\mathbf{P}_x}\right)_i$ is the ith row or column of the matrix square root of $(n_x + \kappa)\mathbf{P}_x$. The weights are normalized (i.e., add up to 1).

2) Propagate each sigma point through the nonlinear function

$$y_i = \mathbf{g}(\chi_i), \qquad i = 0,\ldots 2n_x. \tag{37}$$

3) Estimated mean and covariance of $\mathbf{y}$ are computed as

$$\begin{aligned}
\overline{\mathbf{y}} &= \sum_{i=0}^{2n_x} W_i y_i\\
\mathbf{P}_y &= \sum_{i=0}^{2n_x} W_i (y_i - \overline{\mathbf{y}})(y_i - \overline{\mathbf{y}})^{\mathrm{T}}.
\end{aligned} \tag{38}$$

Next we describe the implementation of the UKF assuming that at time k the state estimate and its covariance are $\hat{\mathbf{s}}_{k|k}$ and $\mathbf{P}_{k|k}$, respectively.

1) Using (36) compute sigma points $\xi_{k|k}(i)$ and weights W_i $(i = 0,\ldots,8)$ corresponding to $\hat{\mathbf{s}}_{k|k}$ and $\mathbf{P}_{k|k}$.

2) Propagate sigma points using state equation (1) as follows

$$\xi_{k+1|k}(i) = \psi_k[\xi_{k|k}(i)] + \mathbf{G}\begin{pmatrix} 0 \\ -g \end{pmatrix}. \tag{39}$$

3) Compute the mean and covariance of the predicted state $\hat{\mathbf{s}}_{k+1|k}$ and $\mathbf{P}_{k+1|k}$ using predicted sigma points $\xi_{k+1|k}(i)$, weights W_i and (38) as follows

$$\begin{aligned}
\hat{\mathbf{s}}_{k+1|k} &= \sum_{i=0}^{8} W_i \xi_{k+1|k}(i)\\
\mathbf{P}_{k+1|k} &= \mathbf{Q} + \sum_{i=0}^{8} W_i [\xi_{k+1|k}(i) - \hat{\mathbf{s}}_{k+1|k}]\\
&\quad \cdot [\xi_{k+1|k}(i) - \hat{\mathbf{s}}_{k+1|k}]^{\mathrm{T}}.
\end{aligned} \tag{40}$$

[3]Recently, it has been published on http://citeseer.nj.nec.comm/julier98reduced.html a new version of unscented transformation that requires just $(n_x + 2)$ sigma points in lieu of $(2n_x + 1)$.

4) Predict measurement sigma points using (10), that is

$$\varsigma_{k+1|k}(i) = \mathbf{H}\boldsymbol{\xi}_{k+1|k}(i). \tag{41}$$

5) Predict measurement and covariances

$$\begin{aligned}
\hat{\mathbf{z}}_{k+1|k} &= \sum_{i=0}^{8} W_i \varsigma_{k+1|k}(i) \\
\mathbf{P}_{zz} &= \mathbf{R}_{k+1} + \sum_{i=0}^{8} W_i [\varsigma_{k+1|k}(i) - \hat{\mathbf{z}}_{k+1|k}] \\
&\quad \cdot [\varsigma_{k+1|k}(i) - \hat{\mathbf{z}}_{k+1|k}]^{\mathrm{T}} \\
\mathbf{P}_{sz} &= \sum_{i=0}^{8} W_i [\boldsymbol{\xi}_{k+1|k}(i) - \hat{\mathbf{s}}_{k+1|k}] \cdot [\varsigma_{k+1|k}(i) - \hat{\mathbf{z}}_{k+1|k}]^{\mathrm{T}}
\end{aligned} \tag{42}$$

where $\mathbf{P}_{zz}$, $\mathbf{P}_{sz}$ are, respectively, the covariance matrix of the measurement and the cross-covariance of the measurement and the state variable.

6) Compute the UKF gain and update state and covariance

$$\begin{aligned}
\mathbf{K}_{k+1} &= \mathbf{P}_{sz}\mathbf{P}_{zz}^{-1} \\
\hat{\mathbf{s}}_{k+1|k+1} &= \hat{\mathbf{s}}_{k+1|k} + \mathbf{K}_{k+1}(\mathbf{z}_{k+1} - \hat{\mathbf{z}}_{k+1|k}) \\
\mathbf{P}_{k+1|k+1} &= \mathbf{P}_{k+1|k} - \mathbf{K}_{k+1}\mathbf{P}_{zz}\mathbf{K}_{k+1}^{T}.
\end{aligned} \tag{43}$$

Note that the UKF requires computation of a matrix square root in (36) which can be done using Cholesky factorisation.

D. Application of Particle Filter

The optimal recursive Bayesian filter of the state vector in the MMSE sense is the mean of the posterior pdf $p(\mathbf{s}_k \mid \mathbf{Z}_k)$. The PF is a computer-based method for implementing an optimal recursive Bayesian filter by Monte Carlo simulations. Instead of analytic solution or numerical approximation of a given nonlinear and/or non-Gaussian problem, it performs a considerable amount of computations in order to approximate the posterior pdf. The central idea is to represent the required pdf by a set of random samples (particles). As the number of particles is increased, the representation of the required pdf becomes more accurate.

The PF in general requires the knowledge of: 1) the initial state pdf $p(\mathbf{s}_0)$; 2) the likelihood function $p(\mathbf{z}_k \mid \mathbf{s}_k)$, and 3) the statistics of process noise $\mathbf{w}_k$. The initial pdf is $p(\mathbf{s}_0) = p_N(\mathbf{s}_0; \hat{\mathbf{s}}_{0|0}, \mathbf{P}_{0|0})$, where $\hat{\mathbf{s}}_{0|0}$ and $\mathbf{P}_{0|0}$ are obtained by two-point differencing method [8, p. 228], [1, p. 253]. From measurement (10), it follows that the likelihood function is Gaussian, $p(\mathbf{z}_k \mid \mathbf{s}_k) = p_N(\mathbf{z}_k; \mathbf{H}\mathbf{s}_k, \mathbf{R}_k)$. As described in Section III, the pdf of process noise is $p(\mathbf{w}_k) = p_N(\mathbf{w}_k; 0, \mathbf{Q})$.

The PF algorithm can be described as follows. Assume that we have a set of random samples (particles) $\Sigma_k = \{\mathbf{s}_k(i) : i = 1, \ldots n\}$ from the posterior density at time k, i.e. $p(\mathbf{s}_k \mid \mathbf{Z}_k)$. The PF is an algorithm for propagating and updating the set of random samples Σ_k to a new set of random samples at time $k+1$, $\Sigma_{k+1} = \{\mathbf{s}_{k+1}(i) : i = 1, \ldots n\}$, which are approximately distributed as the posterior density $p(\mathbf{s}_{k+1} \mid \mathbf{Z}_{k+1})$.

There are several different schemes for carrying out this propagation of random samples, and hence different particle filtering algorithms [7]. In this work we use the sequential importance resampling (SIR) or the bootstrap algorithm [10]. The bootstrap filter propagates the random sample set by the following steps.

1) *Prediction*: Each sample in Σ_k is passed through the state equation (1) to obtain samples from the prior density at time step $k+1$

$$\mathbf{s}_{k+1}^{*}(i) = \psi_k[\mathbf{s}_k(i)] + \mathbf{G}\begin{bmatrix} 0 \\ -g \end{bmatrix} + \mathbf{w}_k(i) \tag{44}$$

where $\mathbf{w}_k(i)$ is a sample drawn from the pdf of process noise $p(\mathbf{w}_k) = p_N(\mathbf{w}_k; 0, \mathbf{Q})$.

2) *Update*: 1) Calculate the likelihood function $p(\mathbf{z}_{k+1} \mid \mathbf{s}_{k+1}^{*}(i))$ for each sample in the set $\Sigma_{k+1}^{*} = \{\mathbf{s}_{k+1}^{*}(i) : i = 1, \ldots n\}$. 2) Calculate the normalized weights for each sample

$$q_{k+1}(i) = \frac{p(\mathbf{z}_{k+1} \mid \mathbf{s}_{k+1}^{*}(i))}{\sum_{j=1}^{n} p(\mathbf{z}_{k+1} \mid \mathbf{s}_{k+1}^{*}(j))}. \tag{45}$$

The weights $q_{k+1}(i)$ represent the probability mass associated with element i of Σ_{k+1}^{*}. 3) Resample n times from the discrete distribution defined by Σ_{k+1}^{*} and $\{q_{k+1}(i) : i = 1, \ldots n\}$ to generate samples $\Sigma_{k+1} = \{\mathbf{s}_{k+1}(i) : i = 1, \ldots, n\}$ so that for any j, $\Pr\{\mathbf{s}_{k+1}(j) = \mathbf{s}_{k+1}^{*}(i)\} = q_{k+1}(i)$.

The MMSE estimate of $\mathbf{s}_{k+1}$ is computed as the mean of particles in Σ_{k+1}:

$$\hat{\mathbf{s}}_{k+1|k+1} = \frac{1}{n}\sum_{i=1}^{n} \mathbf{s}_{k+1}(i). \tag{46}$$

The choice of the number of particles n is very important in the PF design. Note that the SIR algorithm is not particularly efficient (requires large n), because it is resampling from the discrete approximation of the posterior density $p(\mathbf{s}_{k+1} \mid \mathbf{Z}_{k+1})$. Some more recent PF schemes (see [7]) can operate with a smaller number of particles without a significant loss in the estimation accuracy. One such scheme even employs the UT in the prediction step of the PF [19].

VI. NUMERICAL RESULTS

A. Error Analysis

This subsection reports the mean and the standard deviation of the estimation error

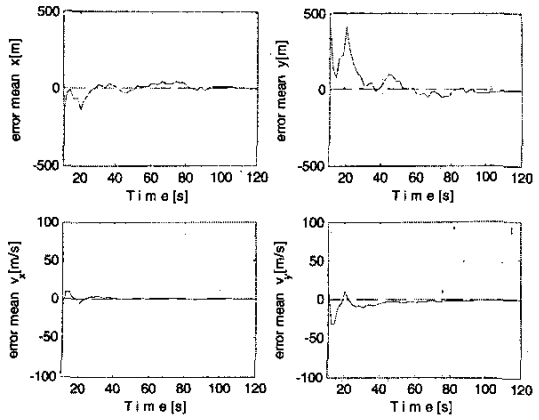

Fig. 4. Mean estimation error of EKF.

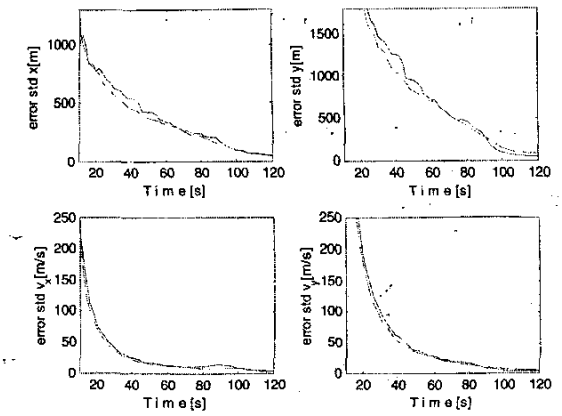

Fig. 5. Errors standard deviation of EKF (solid line) versus square root of theoretical CRLB (dashed line).

$$\mathbf{e}_k = \hat{\mathbf{s}}_{k|k} - \mathbf{s}_k \tag{47}$$

for the four filters described above (EKF, CADET, UKF, and PF, respectively). All performance curves were obtained by averaging over 100 independent Monte Carlo runs. The ballistic target trajectories were generated with the parameters as described in Section III, with $q = 1$. The radar parameters used in simulations were: $T = 2$ s; $\sigma_r = 100$ m and $\sigma_\varepsilon = 0.017$ rad, detection and false alarm probabilities of radar equal to 1 and 0, respectively.

First we present the results obtained using the EKF: the mean of estimation error in target position x and y and velocity $v_x = \dot{x}$ and $v_y = \dot{y}$ is shown in Fig. 4. The standard deviation of error is displayed in Fig. 5.[4]

The Monte Carlo error analysis suggests that the EKF is approximately unbiased with standard deviation just on top of the square root of the CRLB.

Next we present the results on the application of CADET. Figs. 6 and 7 depict the mean and standard deviation of the filtering errors, respectively. As usual, the curves are compared with the CRLB.

In this case the filter is also approximately unbiased with standard deviation close to the square root of the CRLB. The comparison of Figs. 4, 5 with 6, 7 demonstrates that EKF and CADET have very similar performance at least for this study case.

Application of the UKF first requires to select the value of parameter κ. This parameter scales the sigma points of the unscented transformation towards or away from the mean of the prior distribution. If this distribution is Gaussian, Julier, et al. [15] propose to select κ using the following heuristic: $n_s + \kappa = 3$ (because it minimizes the difference between the moments of the standard Gaussian distribution and the sigma points up to fourth order). By following this heuristic one would need to use $\kappa = -1$. Negative κ, however, can cause the calculated covariance to be nonpositive semi-definite. As a compromise we adopted $\kappa = 0$ which produced good results for this application. Figs. 8 and 9 show the UKF error mean and standard deviation, respectively. Similarly to the EKF and CADET, the UKF appears to be statistically efficient (unbiased and attains the CRLB) target state estimator.

As discussed in Section V-D, the PF approximates the optimum recursive Bayesian nonlinear filter; as the number of particles is increased the approximation is more accurate. There are many traps in the implementation of the PF mainly due to the sample impoverishment problem (the number of distinct particles monotonically decreases with time). A simple though costly solution is to use a large number of particles, which is what has been done here: $n = 25000$ particles has been used to obtain the error curves shown in Figs. 10 and 11. These error curves are similar to those obtained by EKF, CADET, and UKF. In summary all four filters show similar error performance: it appears that nonlinearity of the dynamic state equation is not severe for the case when ballistic coefficient β is known.

B. Consistency Tests

All nonlinear filters considered in this study provide, in addition to the state estimates $\hat{\mathbf{s}}_{k|k}$, a self-assessment of their estimation errors. For the EKF, CADET, and UKF this self-assessment is given in the form of the covariance matrix $\mathbf{P}_{k|k}$. The PF provides an estimate of the entire posterior density, from which one can compute both the state estimate as in (46) and its covariance matrix as

$$\mathbf{P}_{k|k} = \frac{1}{n-1}\sum_{i=1}^{n}(\mathbf{s}_k(i) - \hat{\mathbf{s}}_{k|k})(\mathbf{s}_k(i) - \hat{\mathbf{s}}_{k|k})^{\mathrm{T}}. \tag{48}$$

[4]We started the figures from time = 10 s because of the limited performance of the filter initialization.

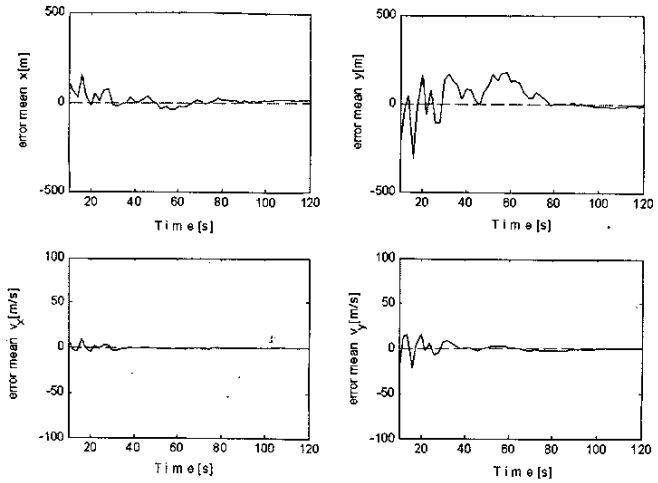

Fig. 6. Mean estimation error of CADET.

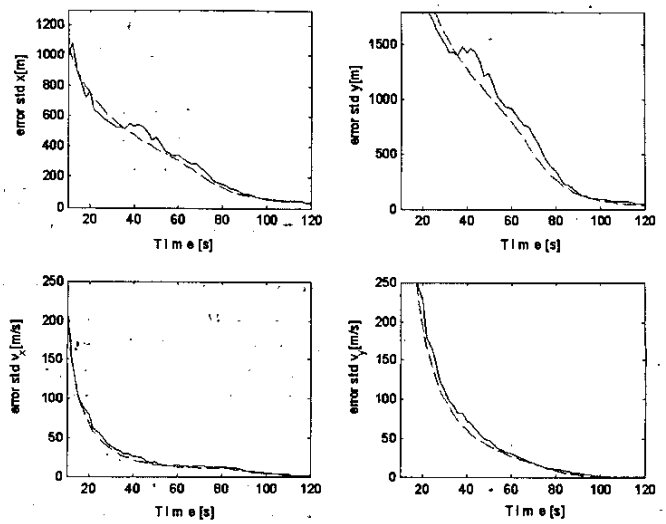

Fig. 7. Errors standard deviation of CADET (solid line) versus square root of theoretical CRLB (dashed line).

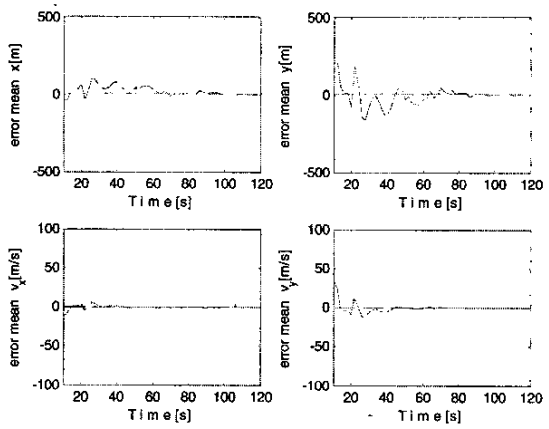

Fig. 8. Mean estimation error of UKF.

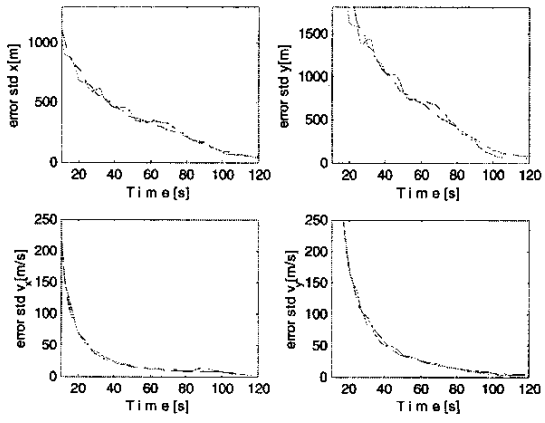

Fig. 9. Errors standard deviation of UKF (solid line) versus square root of theoretical CRLB (dashed line).

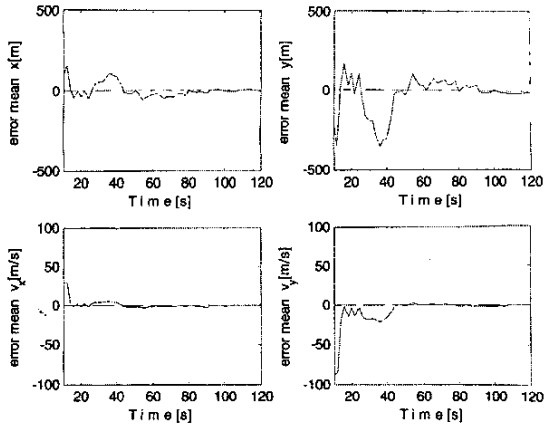

Fig. 10. Mean estimation error of PF.

A filter is referred to as consistent (or credible) if its covariance matrix is equal to the actual mean square error (MSE) matrix [17]. The most common statistical test for filter consistency is the one based on the average normalized estimation error squared (NEES) defined as [1, 17]

$$\bar{\varepsilon}_k = \frac{1}{M \cdot n_s} \sum_{j=1}^{M} [\mathbf{e}_k^j]^{\mathrm{T}} [\mathbf{P}_{k|k}^j]^{-1} \mathbf{e}_k^j \tag{49}$$

where $\mathbf{e}_k^j$ is the error vector defined in (47), with index $j = 1,\ldots M$ denoting the Monte Carlo run, n_s the dimension of the error vector, and M the number of Monte Carlo runs. The consistency test assumes that estimation errors are zero-mean Gaussian. The average NEES of (49) then should be $\chi^2_{n_sM}$ random variable with n_sM degrees of freedom: its mean value is 1 and its variance is $2/n_sM$. The filter is accepted as being consistent (credible) at level α if $\bar{\varepsilon}_k \in [r_1, r_2]$ with probability $1 - \alpha$. The limits of the acceptance interval, r_1 and r_2, are calculated at level $\alpha = 0.05$ (i.e., with probability 0.95) as follows [17]

$$r_{1,2} \approx \frac{1}{2n_sM} \left(\pm 1.96 + \sqrt{2n_sM - 1} \right)^2. \tag{50}$$

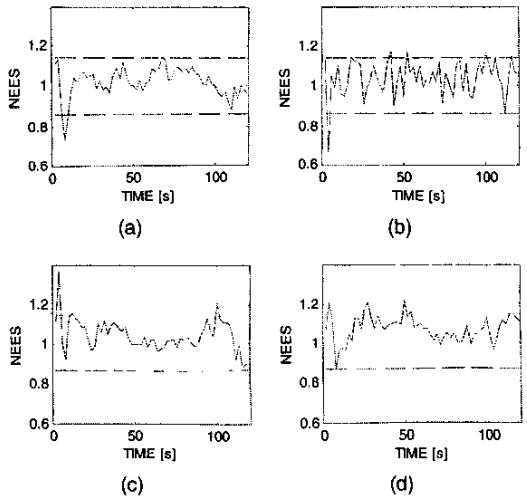

Fig. 12. Average NEES. (a) EKF. (b) CADET. (c) UKF. (d) PF.

The results of the consistency test for EKF, CADET, UKF and the PF are shown in Fig. 12(a), (b), (c), and (d), respectively. The number of Monte Carlo runs is $M = 100$ and $\alpha = 0.05$, which corresponds to the acceptance limits $r_1 = 0.865$ and $r_2 = 1.1421$, indicated in Fig. 12 by horizontal dashed lines. The mean of the estimation error has been removed prior to the calculation of the average NEES [17]. The ballistic target trajectories were generated with the parameters as described in Section III, with $q = 1$. The radar parameters used in simulations as in Sec. VI-A were: $T = 2$ s; $\sigma_r = 100$ m and $\sigma_\varepsilon = 0.017$ rad. Since the total number of scans is 60, the average NEES of a consistent filter is expected to be outside the acceptance interval 5% of time, which

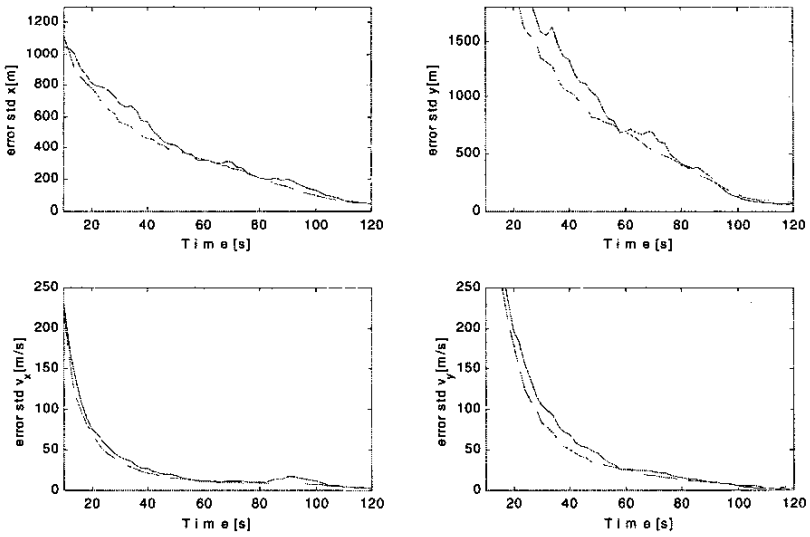

Fig. 11. Errors standard deviation of PF (solid line) versus square root of CRLB (dashed line).

TABLE I
Relative Computational Load

Filter	Relative Computational Load
EKF	1
CADET	300
UKF	3
PF (n = 25000)	440

amounts to 3 scans. The results in Fig. 12 indicate that all four filters are consistent.

VII. CONCLUSIONS

The problem of tracking a ballistic target on reentry has been studied here. Four suboptimum filters have been designed and their performance compared with the theoretical CRLB derived for this estimation problem. From the tracking accuracy point of view, all the four filters (EKF, CADET, UKF, and PF) appear to be statistically efficient (all converge to zero bias with error standard deviation close to the CRLB). Moreover, all four filters produce a credible estimation error self-assessment in form of the filter covariance. In addition to the study case shown in Section VI, the filters have been tested for a wide variety of parameters: standard deviation of radar measurement errors, measurement period T, radar detection probability (also with $P_D < 1$), values of ballistic coefficients β, values of initial target coordinates and speed. The results shown here are representative of several study cases.

The computational complexity of the filters is described in Table I. This table was compiled by measuring the CPU load required for the MATLAB implementation of each of the filters, relative to the CPU load required by the EKF. The conclusion of the study is that EKF is the preferred nonlinear filter for tracking ballistic targets: it combines the statistical efficiency with a modest computational cost.

In the presented study the target ballistic coefficient was assumed to be a known parameter. When β is not known it should be estimated; this topic has recently been studied in [20] and [15] where it was shown that the EKF may diverge. An explanation of the inadequacy of EKF is related to the following: in (8) β appears at the denominator, thus a small estimation error on β will be amplified. In the quoted references it was shown that the preferred filtering solution in terms of performance and computational cost is the UKF which doesn't approximate the nonlinear function.

Topics for future researches are 1) extend the comparison to alternative tracking filters, such the one proposed in [5, 6] and applied to ballistic target tracking in [21]; 2) refine the target kinematics model; 3) study the capability of the trackers to predict the target state ahead in time before the availability of the radar measurements; 4) study the possibility to estimate the launching and landing points of the target from the segment of the ballistic trajectory measured by the radar; it is a matter of how the model of target trajectory fits the reality; if the model is enough accurate and enough measured data are available, in principle it is possible to estimate backwards and ahead of the target trajectory.

ACKNOWLEDGMENTS

The authors acknowledge the excellent editorial work done by Professor P. Willett, Associate Editor for target tracking and multisensor systems of *IEEE Transactions on Aerospace and Electronic Systems.*

REFERENCES

[1] Bar-Shalom, Y., Li, X-R. (1993)
Estimation and Tracking: Principles, Techniques and Software.
Dedham, MA: Artech House, 1993.

[2] Chamberlain, S., Slauenwhite, T. (1993)
United States space command space surveillance network overview.
In *Proceedings of 1st European Conference on Space Debris*, Darmstad, Apr. 1993, 37–42.

[3] Chang, C. B. Whiting, R. H., Athans, M. (1977)
On the state and parameter estimation for maneuvering reentry vehicles.
IEEE Transactions on Automatic Control, **AC-22**, 1 (Feb. 1977), 99–105.

[4] Costa, P. (1994)
Adaptive model architecture and extended Kalman-Bucy filters.
IEEE Transactions on Aerospace and Electronic Systems, **AES-30**, 2 (Apr. 1994), 525–533.

[5] Daum, F. E. (1986)
Exact finite dimensional nonlinear filters.
IEEE Transactions on Automatic Control, **AC-31**, 7 (July 1986), 616–622.

[6] Daum, F. E. (1995)
Beyond Kalman filters: Practical design of nonlinear filters.
Proceedings of SPIE, **2561** (1995), 252–262.

[7] Doucet, A., de Freitas, N., Gordon, N. J. (Eds.)
Sequential Monte Carlo Methods in Practice.
New York: Springer-Verlag, Jan. 2001.

[8] Farina, A. Studer, F. A. (1985)
Radar Data Processing. Introduction and Tracking, Vol. I.
England: Researches Studies Press, May 1985.

[9] Gelb, A. (1974)
Applied Optimal Estimation.
Cambridge MA: M.I.T. Press, 1974, pp. 216–224.

[10] Gordon, N. J., Salmond, D. J., Smith, A. F. M. (1993)
Novel approach to nonlinear/non-Gaussian Bayesian state estimation.
IEE Proceedings, Pt. F. **140**, 2 (Apr. 1993), 107–113.

[11] Hutchins, R., San Jose, A. (1998)
IMM tracking of a theater ballistic missile during boost phase.
In *Proceedings of SPIE Conference on Signal and Data Processing of Small Targets* (SPIE vol.3373), Orlando, FL, Apr. 1998, 528–537.

[12] Kalman, R. E., Bucy, R. S. (1961)
New results in linear filtering and prediction theory.
Journal of Basic Engineering, **83** (1961), 95–108.

[13] Jazwinski, A. H. (1970)
Stochastic Processes and Filtering Theory.
New York: Academic Press, 1970.

[14] Julier, S. Uhlmann, J. (1997)
A new extension of the Kalman filter to nonlinear systems.
In *The Proceedings of AeroSense: The 11th International Symposium on Aerospace/Defense Sensing, Simulation and Controls*, Orlando, FL, 1997; (Multi Sensor Fusion, Tracking and Resource Management II, SPIE vol. 3068, pp.182–193).

[15] Julier, S. Uhlmann, J., Durrant-Whyte, H. F. (2000)
A new method for the non linear transformation of means and covariances in filters and estimators.
IEEE Transactions on Automatic Control, **AC-45**, 3 (Mar. 2000), 477–482.

[16] Lerro, D., Bar-Shalom, Y. (1993)
Tracking with debiased consistent converted measurements vs. EKF.
IEEE Transactions on Aerospace and Electronic Systems, **29**, 3 (July 1993), 1015–1022.

[17] Li, X. R., Zhao, Z., Jilkov, V. P. (2001)
Practical measures and test for credibility of an estimator.
In *Proceedings of the Workshop on Estimation, Tracking and Fusion: A Tribute to Y. Bar-Shalom*, Monterey, CA, May 2001, 481–495.

[18] Mehra, R. (1971)
A comparison of several non-linear filters for re-entry vehicle tracking.
IEEE Transactions on Automatic Control, **AC-16**, 4 (Aug. 1971), 307–319.

[19] van der Merwe, R., Doucet, A., de Freitas, N., Wan, E. (2000)
The unscented particle filter.
Technical report CUED/F-INFENG/TR 380, Cambridge University, Eng. Dept, 2000.

[20] Ristic, B., Farina, A., Benvenuti, D. (2002)
Tracking a ballistic re-entry object: Performance bounds and comparison of non-linear filters.
IDC-2002, Adelaide, Australia, 11–13 February, 2002, 259–264.

[21] Schmidt, G. C. (1993)
Designing nonlinear filters based on Daum's theory.
Journal of Guidance, Control and Dynamics, 16,i2 (Mar.–Apr. 1993), 371–376.

[22] Taylor, J. H. (1979)
The Cramer-Rao estimation error lower bound computation for deterministic nonlinear systems.
IEEE Transactions on Automatic Control, **AC-24**, 2 (Apr. 1979), 343–344.

[23] Tichavsky, P., Muravchik, C. H., Nehorai, A. (1998)
Posterior Cramer-Rao bounds for discrete-time nonlinear filtering.
IEEE Transactions on Signal Processing, **46**, 5 (May 1998), 1386–1395.

[24] Van Trees, H. (1968)
Detection, Estimation and Modulation Theory.
New York: Wiley, 1968.

[25] Zarchan, P. (1997)
Tactical and Strategic Missile Guidance (3rd ed.).
AIAA, Progress in Astronautics and Aeronautics, vol. 176, 1997.

Alfonso Farina (M'85–SM'97—F'00) received his doctor degree in electronic engineering from the University of Rome (I) in 1973.

In 1974 he joined Selenia, now Alenia Marconi Systems, where he is a manager (since May 1988) in the Technical Directorate of Radar & Technology Division. Since 1979, he has also been Professore Incaricato of Radar Techniques at the University of Naples; in 1985 he was appointed Associate Professor.

Dr. Farina is the author of more than 240 peer reviewed publications and the author of books and monographs: *Radar Data Processing* (Vol. 1 and 2), 1985–1986; *Optimised Radar Processors*, 1987; *Antenna Based Signal Processing Techniques for Radar Systems*, 1992. He has written chapter 9 on "ECCM techniques" in the Radar Handbook (2nd edition 1990), edited by Dr. M. I. Skolnik of Naval Research Laboratory. He has been session chairman at many international radar conferences. He used to lecture at universities and research centers in Italy and abroad; he also frequently gives tutorials at the Intl. Radar Conferences on signal, data and image processing for radar; in particular on multi-sensor fusion, adaptive signal processing, space time adaptive processing (STAP) and detection. In the 1987 He received the Radar Systems Panel Award of IEEE-AESS for development of radar data processing techniques. He is the Italian representative at the International Radar Systems Panel of IEEE-AESS. He has been the Italian industrial representative at the SET (Sensor and Electronic Technology) of RTO (Research Technology Organisation) of NATO. He has been in the BoD of the International Society for Information Fusion (ISIF). Recently has been nominated Fellow of IEEE with the following citation: "For development and application of adaptive signal processing methods for radar systems." He is a referee of numerous publications submitted to several Journals of IEE, IEEE and EURASIP, He also cooperates with the editorial board of ECEJ (Electronics & Communication Engineering Journal) of IEE. He is a Fellow of IEE.

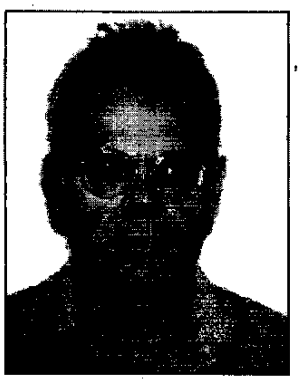

Branko Ristic received his first two degrees in Yugoslavia: B.Eng. from the University of Novi Sad in 1984 and M.Sc. from Belgrade University in 1991, both in electrical engineering. He received the Ph.D. degree from the Signal Processing Research Centre at QUT in Brisbane, Australia, in 1995.

Between 1984 and 1988 he was a Research Assistant at The University of Novi Sad. In February 1989 he was initially a Senior Research Assistant at The Queensland University (1989–1991) and then at QUT (1991–1993). During 1995 he was a Senior DSP Engineer in GEC Marconi Systems (Sydney, Australia) and in 1996 he joined Defence Science and Technology Organisation (DSTO) as research scientist. Currently he is a Senior Research Scientist in the Surveillance Systems Division of DSTO responsible for algorithm development and performance analysis of tracking and multi-sensor integration systems. His main research interests currently include estimation theory, target tracking and non-linear filtering.

Dario Benvenuti was born in Rome the 29 October 1971. He graduated in electronic engineering at the University of Rome "La Sapienza" in 1998.

He served as lieutenant in the Italian Army in 1997. In 1999 he joined the Technical Directorate (Radar & Technology Division) of Alenia Marconi Systems. His working activities are dedicated to the analysis and system aspects of a modern multifunctional phased-array radar system. Since 2000 Dario is attending a course for a laurea degree in physics at the University of Rome.